Response to Reviewer comment #3:

General comments:

This paper presents measurements of OH and HO_2 radicals during the STORM campaign in the Pearl River Delta and compare their measurements to model predictions. The authors conclude that the model underestimates the measured OH concentration but can reproduce the measured HO2 concentrations. The authors propose that the "X" mechanism can explain the discrepancy, similar to that proposed in previous studies. The proposed mechanism involves an unmeasured species "X" that converts RO_2 to HO_2 and HO_2 to OH similar to NO. The authors conclude that a mixing ratio of "X" equivalent to 0.1 ppb of NO is needed to bring the measured OH concentrations into agreement with the measurements.

However, it is not clear that their measurements support their conclusion that the model significantly underestimates the measured concentrations, as it appears that the model agrees with the measurements to within the uncertainty of the technique. This is in contrast to the previous measurements highlighted in the paper, where the discrepancy between models and measurements were found to be much greater, such as the factor of 3-5 found by Hofzumahaus et al. (2009). While the addition of the X mechanism does improve the agreement with the measurements, there is no discussion as to why the measurements reported here are in better agreement with the model compared to the previous measurements discussed in the paper. The paper would benefit from an expanded discussion of the measurement-model agreement taking the uncertainties associate with both into account. In addition, the paper would benefit from an expanded discussion of a comparison of their results with the previous measurements mentioned in the manuscript, especially the difference between their measurements and those at the Backgarden and Heshan sites in the PRD (Hofzumahaus et al., 2009; Tan et al., 2019). Such a discussion could provide more information about the source of the model-measurement discrepancies at all these sites.

The measurements of OH and HO_2 appear to be high quality and are of interest to the atmospheric chemistry community. In addition to addressing the major comment described above, I believe the paper would be publishable after the authors also address the following in a revised manuscript.

Reply

Thanks for your critical comments and suggestions concerning our manuscript. We have studied all the comments which were helpful for revising and improving our manuscript. We have made corrections which we hope meet with approval. Below are our responses to the specific comments, highlighted in blue, with changes to the manuscript highlighted in green.

Specific comments:

1. The authors state that the base model agrees with the measurements to within the uncertainties of the measurements and the model (line 177), but then states that the model underestimates the measurements after 10 am when NO decreases. However, based on the information provided in Figure 3a, it appears that the model still agrees with the measurements to within the combined uncertainty of both the model and the measurements. This should be clarified. Addition of uncertainty estimates in Figure 3 would help to illustrate the agreement.

Reply

We recheck the data (details in the Reply to Question 4) and added the uncertainty of radical concentrations in fig. 3 as your suggestions. The description of the comparison between the observed and modeled radical concentrations was revised in Section 3.2.

Revision

Section 3.2:

The observed and modeled OH concentrations agreed within their 1-σ uncertainties of measurement and simulation (11% and 40%). However, when the NO mixing ratio (Fig. 2) dropped from 10:00 gradually, a systematic difference existed, with the observed OH concentration being about 1×10^6 cm^{-3} higher than the modeled OH concentration.

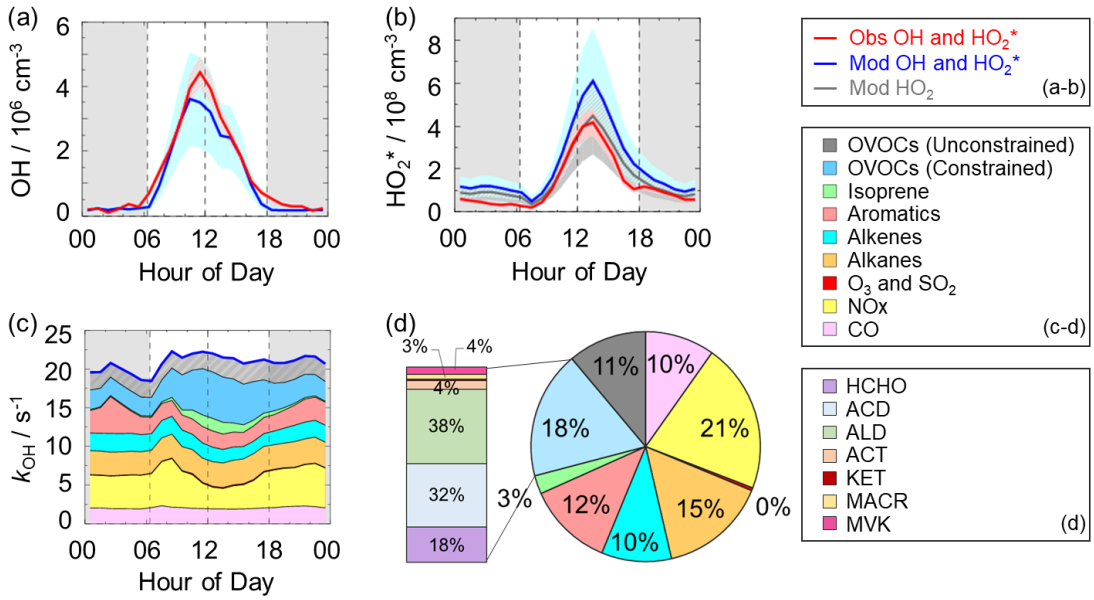

Figure 3: (a-b) The diurnal profiles of the observed and modeled OH, HO_2^* and HO_2 concentrations. (c) The diurnal profiles of the modeled k_{OH}. (d) The composition of the modeled k_{OH}. The red areas in (a-b) denote 1-σ uncertainties of the observed OH and HO_2^* concentrations. The blue areas in (a-b) denote 1-σ uncertainties of the modeled OH and HO_2^* concentrations, and the grey area in (b) denotes 1-σ uncertainties of the modeled HO_2 concentrations. The grey areas in (a-c) denote nighttime. ACD denotes acetaldehydes. ALD denotes the C3 and higher aldehydes. ACT and KET denote acetone and ketones. MACR and MVK denote methacrolein and methyl vinyl ketone.

2. Similarly, the base model predictions at low NO shown in Figure 5, although lower than the median measurements, appear to be within the combined uncertainty of model and measurements. The authors should quantify the discrepancy between the measurements and the model at each NO bin and reassess whether there is significant disagreement at low NO.

Reply

Thanks for your suggestions. The box-whisker plots in Fig. 5 denote the 10%, 25%, median, 75%, and 90% of HOx observations during the whole campaign rather than the 1-σ uncertainty of HOx observations. Herein, we compared the daily median of the observed and modeled OH concentrations with 1-σ uncertainty under the low NO intervals during the noontime (< 0.2 ppb, 0.2-0.6 ppb) in the following figure. The medium modeled OH concentrations were lower than the medium observed concentrations on most days. When we considered the combined uncertainty of OH observations (11%) and simulation (40%), the modeled OH concentrations were still lower than the OH observations on several days, especially when NO concentration was below 0.2 ppb.

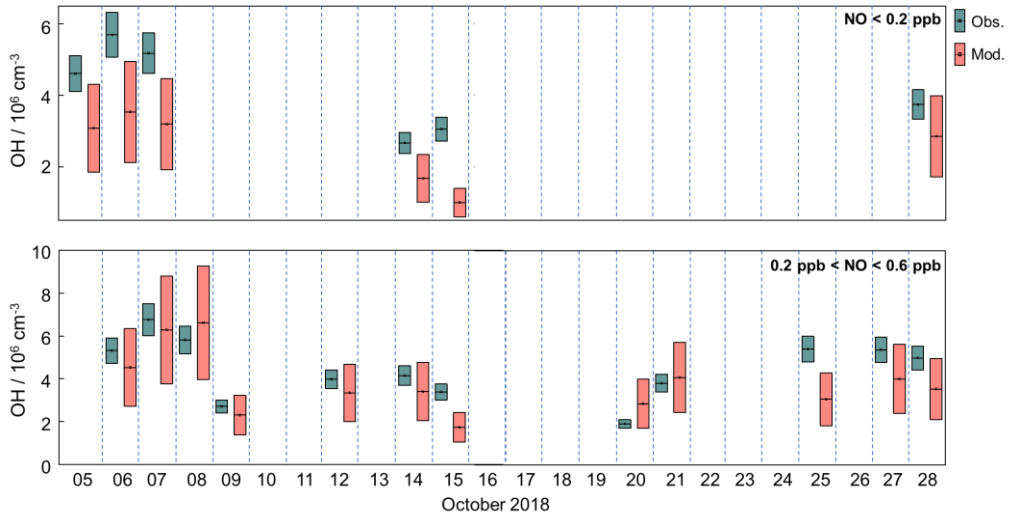

Figure: The daily median of the observed and modeled OH concentration with 1-σ uncertainty under the low NO intervals (< 0.2 ppb, 0.2-0.6 ppb) during the noontime.

Additionally, we further explored the composition of VOCs reactivity under the different NO intervals, as shown in the revised Fig. 5.

Revision

(1) Section 4.2.1:

To further explore the influencing factors of OH underestimation, we presented the speciation VOCs reactivity under the different NO intervals, as shown in Fig. 5 and Table S4 in the Supplementary Information. The isoprene reactivity and total OVOCs reactivity (the sum of HCHO, ACD, ACT, ALD, KET, MACR, MVK and the modeled OVOCs) increased with the decrease of NO concentrations, while the anthropogenic VOCs reactivity (alkanes, alkenes and aromatics) was higher in high NO regime. Additionally, the O_3 concentration in low NO regime was significantly higher than those in high NO regime, and the temperature was slightly higher in low NO regime, demonstrating the photochemistry was more active in low NO regime in

this campaign. Overall, the photochemistry and composition of VOCs reactivity, especially the isoprene and OVOCs species (mainly ACD, ACT and the modeled OVOCs), might closely impact the missing OH sources.

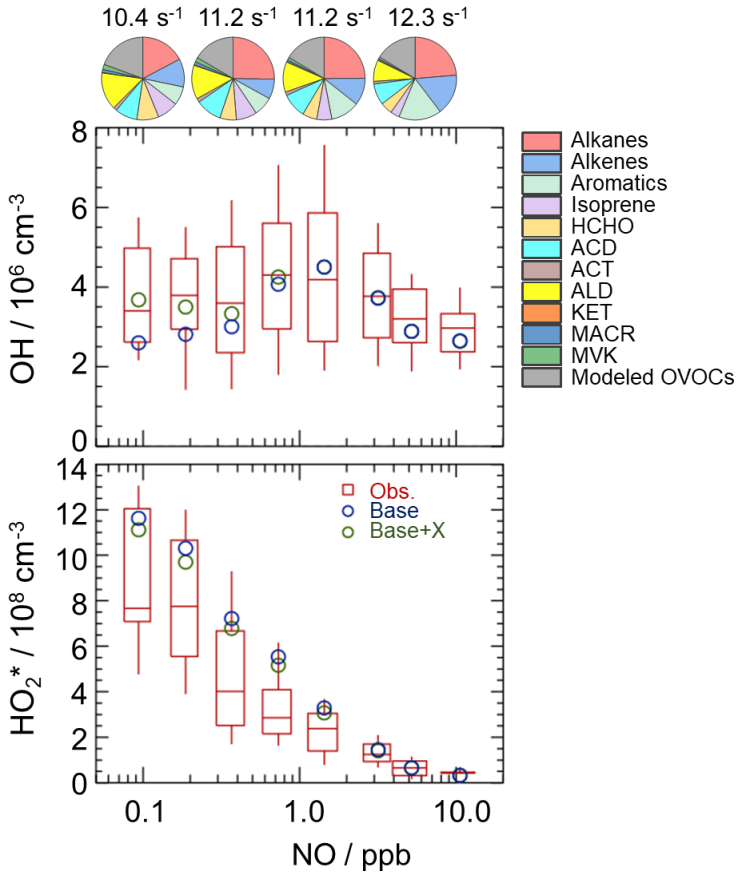

Figure 5: NO dependence of OH and HO_2^* radicals. The red box-whisker plots give the 10%, 25%, median, 75%, and 90% of the HOx observations. The blue circles show the median values of the HOx simulations by the base model, and the green circles show the HOx simulations by the model with X mechanism. Total VOCs reactivities and their organic speciation are presented by pie charts at the different NO intervals at the top. Only daytime values and NO concentration above the detection limit of the instrument were chosen. ACD and ACT denote acetaldehyde and acetone, respectively. ALD denotes the C3 and higher aldehydes. KET denotes ketones. MACR and MVK, which are both the isoprene oxidation products, denote methacrolein and methyl vinyl ketone, respectively.

(2) The median values of meteorological and chemical parameters during the daytime at the different NO intervals were added in Table S4 in the Supplementary Information:

Table S4: The median values of meteorological and chemical parameters during the daytime at the different NO intervals.

parameters	NO interval (< 0.2 ppb)	NO interval (0.2-0.6 ppb)	NO interval (0.6-2 ppb)	NO interval (> 2 ppb)
Temperature / K	301.4	300.8	299.1	297.9
$j(O^1D)$ / 10^{-6} s^{-1}	4.7	8.9	8.2	7.4
O_3 concentration / ppb	71.7	55.1	39.6	16.9

Alkanes reactivity / s^{-1}	2.2	3.4	3.3	3.5
Alkenes reactivity / s^{-1}	1.4	1.0	1.4	2.3
Aromatics reactivity / s^{-1}	0.9	1.0	1.5	2.4
Isoprene reactivity / s^{-1}	1.1	1.1	0.8	0.5
HCHO reactivity / s^{-1}	1.1	0.9	0.8	0.7
ACD reactivity / s^{-1}	1.1	1.4	1.3	1.2
ACT reactivity / s^{-1}	0.2	0.2	0.2	0.2
ALD reactivity / s^{-1}	1.9	1.8	1.6	1.2
KET reactivity / s^{-1}	0.0	0.0	0.0	0.0
MACR reactivity / s^{-1}	0.2	0.2	0.1	0.1
MVK reactivity / s^{-1}	0.3	0.2	0.1	0.1
Modeled OVOCs reactivity / s^{-1}	2.5	2.2	2.2	2.4
Alkanes concentration / ppb	15.0	16.8	19.0	24.6
Alkenes concentration / ppb	1.6	1.6	2.0	3.4
Aromatics concentration / ppb	3.3	3.3	4.8	7.9
Isoprene concentration / ppb	0.4	0.4	0.3	0.2
HCHO concentration / ppb	5.6	4.3	3.8	3.5
ACD concentration / ppb	3.0	3.7	3.5	3.3
ACT concentration / ppb	3.2	3.7	3.3	2.7
ALD concentration / ppb	3.8	3.6	3.2	2.5
KET concentration / ppb	0.3	0.4	0.4	0.3
MACR concentration / ppb	0.2	0.2	0.1	0.1
MVK concentration / ppb	0.5	0.5	0.3	0.2

3. The analysis of the OH measurements assumes that there are no interferences associated with the LIF-FAGE measurements. However, there is no discussion of whether the authors tested for unknown interferences with their measurements through a chemical modulation technique similar to that described in Tan et al. (2019). This should be addressed, as a significant interference would suggest that the model overestimation of OH could be more significant.

Reply

Thanks for your suggestions, the pre-injector system really did not be applied in this campaign, and it would introduce uncertainty into the OH measurement. However, it is believed that the interference in OH measurement in this campaign was negligible by analyzing the

PKU-LIF system and the environmental conditions during the campaign.

PKU-LIF system has been used to measure HOx concentrations since 2014. We used the pre-injector system to quantify the possible interferences for several campaigns, including the campaigns conducted in Wangdu site (Tan et al., 2017), Heshan site (Tan et al., 2019), Huairou site (Tan et al., 2018), Taizhou (Ma et al., 2022, in review, ACPD), and Chengdu site (Yang et al., 2021). No significant internal interference was found in the prior studies, demonstrating the accuracy of the PKU-LIF system has been determined several times.

Moreover, the potential interference may exist when the sampled air contained alkenes, ozone, and BVOCs (Mao et al., 2012; Fuchs et al., 2016; Novelli et al., 2014), indicating the environmental conditions, especially O_3, alkenes and isoprene, are important to the OH interferences. To further explore the potential interference in this campaign, we take Wangdu campaign as an example to compare the major environmental conditions between the prior campaigns and Shenzhen campaign here. During the Wangdu campaign, the chemical modulation tests were conducted on 29 June, 30 June, 02 July, and 05 July 2014, respectively (Tan et al., 2017). The daily mean O_3, alkenes (ethene, butadiene and other anthropogenic dienes, internal alkenes and terminal alkenes) and isoprene concentrations during the daytime on 29 June were 94.1, 3.8, 1.9 ppb, those on 30 June were 92.2, 2.7, and 1.9 ppb, those on 02 July were 52.9, 1.5, and 0.5 ppb, and those on 05 July were 68.5, 2.4, and 0.9 ppb. The O_3, alkenes and isoprene concentrations on 29 June were highest among those on 29 June, 30 June, 02 July and 05 July, and thus the potential interference on 29 June can be considered the highest among the four days. The results indicated that the potential interference during the daytime in Wangdu was negligible.

Here, we also showed the major parameters related to OH interference in Shenzhen in Table S2 in the Supplementary Information. The daily mean O_3 and isoprene concentrations during the daytime in Shenzhen were within 8.6-91.7 ppb and 0.1-1.0 ppb, which were both lower than those on 29 June in Wangdu. In terms of the alkenes, only 10,16-17 October 2018 in Shenzhen campaign were higher than that observed on 29 June in Wangdu, but the O_3 concentrations on the three days in Shenzhen were only 21.9, 13.9, and 8.6 ppb, and the isoprene concentrations on the three days in Shenzhen were only 0.3, 0.2, and 0.1 ppb, respectively. Overall, the environmental condition in Shenzhen was less conducive to generating potential OH interference than that in Wangdu. Therefore, it is not expected that OH measurement in this campaign was affected by the internal interference.

We have added the description of interval interference in Section 2.2 and the Supplementary Information.

Table S2: The daily mean O_3, alkenes (ethene, butadiene and other anthropogenic dienes, internal alkenes and terminal alkenes) and isoprene concentrations during the daytime (08:00-17:00) in the STORM campaign in this study.

Date / Species	10-05	10-06	10-07	10-08	10-09	10-10	10-11	10-12	10-13	10-14	10-15	10-16
O_3 (ppb)	81.4	83.8	91.7	86.7	48.1	21.9	30.2	42.6	46.8	38.7	40.2	13.9
Alkenes (ppb)	1.4	1.8	3.6	2.3	3.2	5.4	2.9	2.4	2.6	1.4	1.6	4.9
Isoprene (ppb)	0.4	0.4	0.4	0.5	0.4	0.3	0.1	0.3	0.4	0.4	0.6	0.2

Date / Species	10-17	10-18	10-19	10-20	10-21	10-22	10-23	10-24	10-25	10-26	10-27	10-28
O_3 (ppb)	8.6	16.2	39.4	45.8	47.2	25.2	40.9	36.5	55.2	56.5	60.9	60.8
Alkenes (ppb)	4.7	3.2	2.1	1.3	1.2	2.5	2.9	2.7	1.2	3.4	1.7	1.7
Isoprene (ppb)	0.1	0.1	0.5	0.3	0.8	0.8	0.4	0.3	0.5	1.0	0.6	0.8

Revision

(1) Section 2.2:

Additionally, prior studies reported that OH measurement might be affected by the potential interference, when the sampled air contained ozone, alkenes and BVOCs (Mao et al., 2012; Fuchs et al., 2016; Novelli et al., 2014), indicating the environmental conditions are important to the production of interference. The pre-injector is usually used to test the potential OH interference, and has been applied to our PKU-LIF system to quantify the possible interferences for several campaigns, including the campaigns conducted in Wangdu, Heshan, Huairou, Taizhou and Chengdu sites (Tan et al., 2017; Tan et al., 2019; Tan et al., 2018; Yang et al., 2021). No significant internal interference was found in the prior studies, demonstrating the accuracy of the PKU-LIF system has been determined for several times. Moreover, to further explore the potential interference in this campaign, we compared the major environmental conditions, especially O_3, alkenes and isoprene, between Shenzhen and Wangdu sites, as shown in the Supplementary Information. The environmental condition in Shenzhen was less conducive to generating interference than that in Wangdu, and the details were presented in the Supplementary Information. Therefore, it is not expected that the OH measurements in this campaign were affected by the internal interference.

(2) The detailed information on potential OH interference was added in the Supplementary Information:

We compared the environmental conditions in Shenzhen and Wangdu sites. The chemical modulation tests, which was applied to test the potential OH interference, were conducted on 29 June, 30 June, 02 July and 05 July 2014 in Wangdu (Tan et al., 2017). During the campaign in Wangdu, the daily mean O_3, alkenes (ethene, butadiene and other anthropogenic dienes, internal alkenes and terminal alkenes) and isoprene concentrations during the daytime on 29 June were 94.1, 3.8, 1.9 ppb, those on 30 June were 92.2, 2.7, and 1.9 ppb, those on 02 July were 52.9, 1.5, and 0.5 ppb, and those on 05 July were 68.5, 2.4, and 0.9 ppb, respectively. The O_3, alkenes and isoprene concentrations on 29 June were the highest among those on 29 June, 30 June, 02 July and 05 July, and thus the potential interference on 29 June can be considered the highest among the four days. The chemical modulation results indicated that the potential interference during the daytime in Wangdu was negligible (Tan et al., 2017).

As shown in Table S2, the O_3, alkenes and isoprene concentrations in Shenzhen were within 8.6-91.7 ppb, 1.2-5.4 ppb, and 0.1-1.0 ppb, respectively. The O_3 concentrations in Shenzhen (8.6-91.7 ppb) were lower than those on 29 June (94.1 ppb) and 30 June (92.2 ppb) in Wangdu. Similarly, the isoprene concentrations in Shenzhen (0.1-1.0 ppb) were also lower than those on

29 June (1.9 ppb) and 30 June (1.9 ppb) in Wangdu. In terms of the alkenes, only the concentrations on 10, 16-17 October 2018 (4.7-5.4 ppb) in Shenzhen were higher than that observed on 29 June (3.8 ppb) in Wangdu, but the O_3 concentrations on the three days in Shenzhen were only 21.9, 13.9, and 8.6 ppb, and the isoprene concentrations on the three days in Shenzhen were only 0.3, 0.2, and 0.1 ppb, respectively.

Overall, the environmental condition in Shenzhen was less conducive to generating potential OH interference than that in Wangdu. Therefore, it is not expected that OH measurement in this campaign was affected by the internal interference.

4. I assume that the higher NO flow that was used in the HO_2 measurements was required to increase the signal to allow for adjusting the laser wavelength given the failure of the reference cell. Were these measurements included in the data? While the authors claim that the NO concentrations were still low enough to minimize RO_2 conversion to OH, did the authors perform calibrations of some RO_2 conversion efficiencies to confirm this? What HO_2 to OH conversion efficiencies did these two NO flows correspond to? Providing more details on the potential for RO_2 interferences with the HO_2 measurements would improve the reader's confidence in the measurements.

Reply

Thanks for your helpful suggestions. We have rechecked all the data and made corrections in the revised manuscript.

Revision:

(1) Section 2.2:

In this campaign, NO mixing ratios were switched between 25 ppm (low NO mode) and 50 ppm (high NO mode). We calculated the HO_2 conversion rates under the two different NO concentrations by calibrating the PKU-LIF system. HO_2 conversion rates in low NO mode ranged within 80%-95%, while those in high NO mode were over 100%, demonstrating that the HO_2 measurement was affected by RO_2 radicals. Prior studies have reported the relative detection sensitivities (α_{RO_2}) for the major RO_2 species, mainly from alkenes, isoprene and aromatics, when the HO_2 conversion rate was over 100% (Fuchs et al., 2011; Lu et al., 2012; Lu et al., 2013). Therefore, only the HO_2 observations in high NO mode were chosen and they were denoted as $[HO_2^*]$, which was the sum of the true HO_2 concentration and a systematic bias from the mixture of RO_2 species *i* which were detected with different relative sensitivities $\alpha^i_{RO_2}$, as shown in Eq. (1) (Lu et al., 2012). The true HO_2 concentration was difficult to calculated due to the RO_2 concentration measurements and their speciation were not available. Herein, we simulated the HO_2 and HO_2^* concentrations by the model. The interference from RO_2 was estimated to be the difference between the HO_2 and HO_2^* concentrations.

$$[HO_2^*] = [HO_2] + \sum(\alpha^i_{RO_2} \times [RO_2]_i) \quad (1)$$

(2) The figures and descriptions of HO_2 concentration were revised in Section 3.2:

The diurnal maximum of the observed HO_2^*, the modeled HO_2^* and the modeled HO_2 concentrations were 4.2×10^8 cm^{-3}, 6.1×10^8 cm^{-3}, and 4.4×10^8 cm^{-3}, respectively. The difference between the modeled HO_2^* and HO_2 concentrations can be considered a modeled HO_2 interference from RO_2 (Lu et al., 2012). The RO_2 interference was small in the morning, while it became larger in the afternoon. It ranged within 23%-28% during the daytime (08:00-17:00), which was comparable with those in the Backgarden and Yufa sites in China, Borneo rainforest in Malaysia (OP3 campaign, aircraft), and UK (RONOCO campaign, aircraft) (Lu et al., 2012; Lu et al., 2013; Jones et al., 2011; Stone et al., 2014). The observed HO_2^* was overestimated by the model, indicating the HO_2 heterogeneous uptake might have a significant impact during this campaign. The diurnal maximum of HO_2^* concentration observed in Shenzhen was much lower than those observed in the Yufa and Backgarden sites (Hofzumahaus et al., 2009; Lu et al., 2012; Lu et al., 2013).

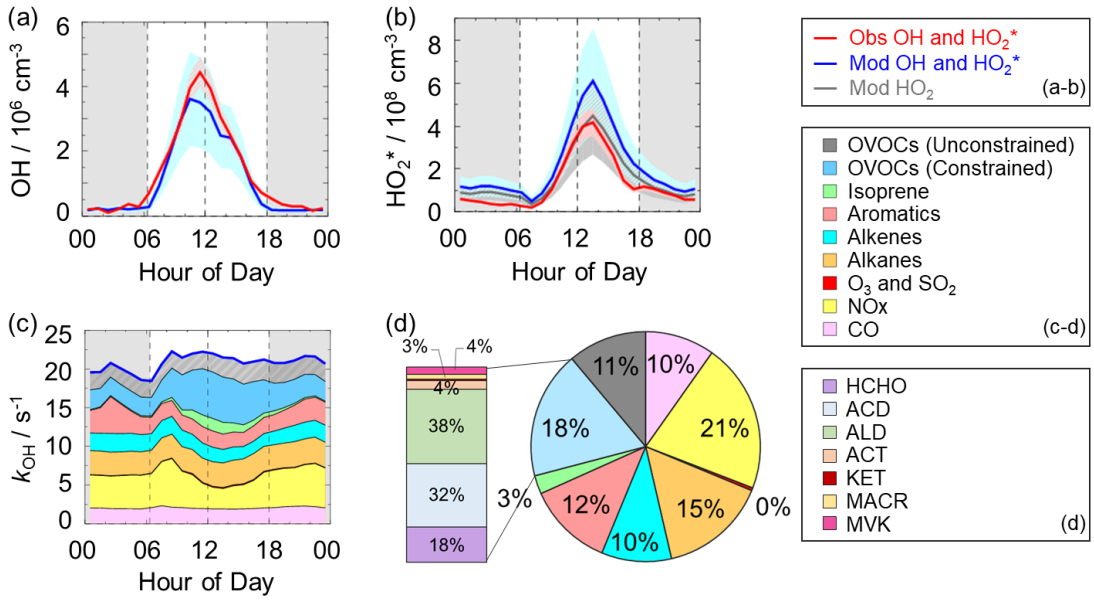

Figure 3: (a-b) The diurnal profiles of the observed and modeled OH, HO_2^* and HO_2 concentrations. (c) The diurnal profiles of the modeled k_{OH}. (d) The composition of the modeled k_{OH}. The red areas in (a-b) denote 1-σ uncertainties of the observed OH and HO_2^* concentrations. The blue areas in (a-b) denote 1-σ uncertainties of the modeled OH and HO_2^* concentrations, and the grey area in (b) denotes 1-σ uncertainties of the modeled HO_2 concentrations. The grey areas in (a-c) denote nighttime. ACD denotes acetaldehydes. ALD denotes the C3 and higher aldehydes. ACT and KET denote acetone and ketones. MACR and MVK denote methacrolein and methyl vinyl ketone.

(3) The timeseries of HO_2 concentrations were revised in Figure S1:

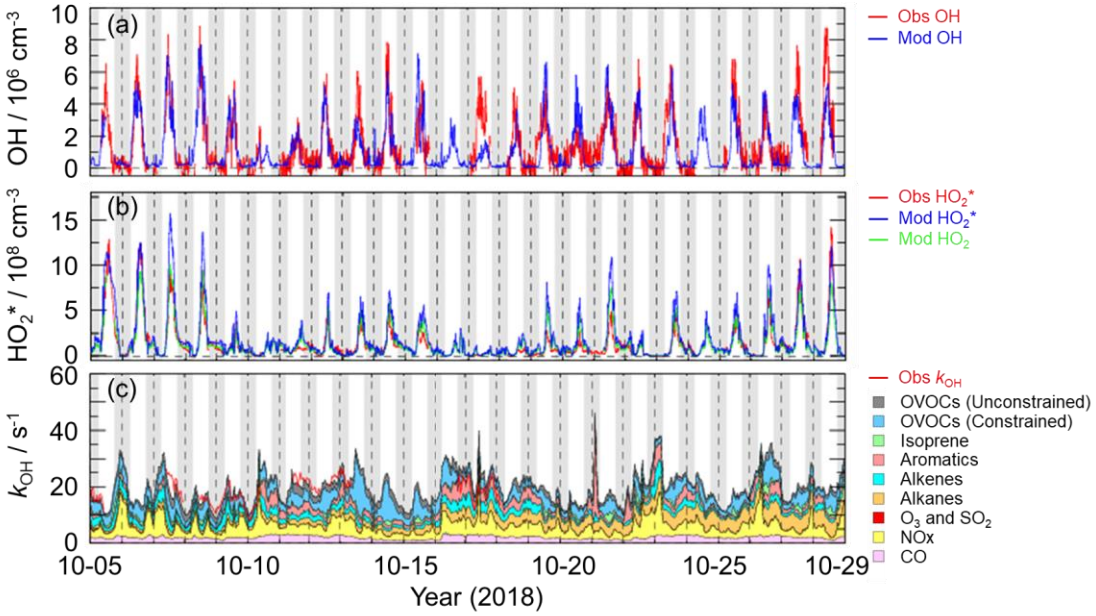

Figure S1: Timeseries of the OH, HO_2^*, HO_2 concentrations and k_{OH} in this study. The grey areas denote nighttime.

(4) The observed HO_2 concentrations can influence the OH experimental budget, so the description in Section 4.1 was revised:

It is noted that the OH production rate was overestimated because we used HO_2^* concentrations instead of HO_2 concentrations here. Thus, the missing OH source was the lower limit here, demonstrating more unknown OH sources need to be further explored.

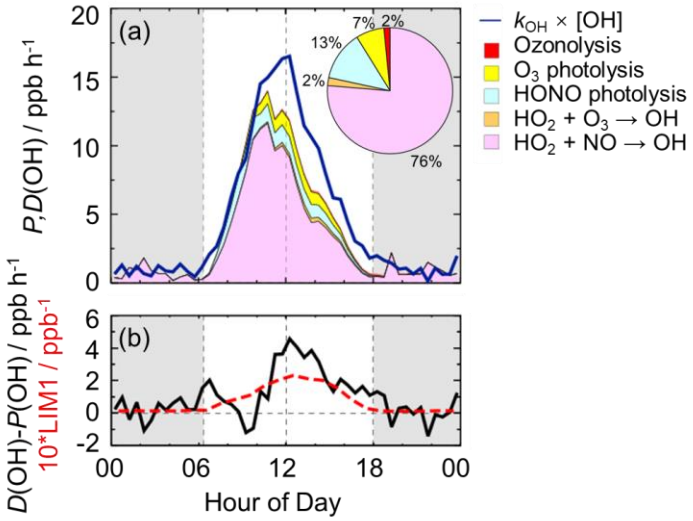

Figure 4: (a) The diurnal profiles of OH production and destruction rates and the proportions of different known sources in the calculated production rate during the daytime. The blue line denotes the OH destruction rate, and the colored areas denote the calculated OH production rates from the known sources. (b) The missing OH source which was the discrepancy between the OH destruction and production rates, and the OH production rate which was ten times the production rate derived from LIM1 mechanism. The grey areas denote nighttime.

(5) The NO dependence of HOx radicals in Fig. 5 was revised:

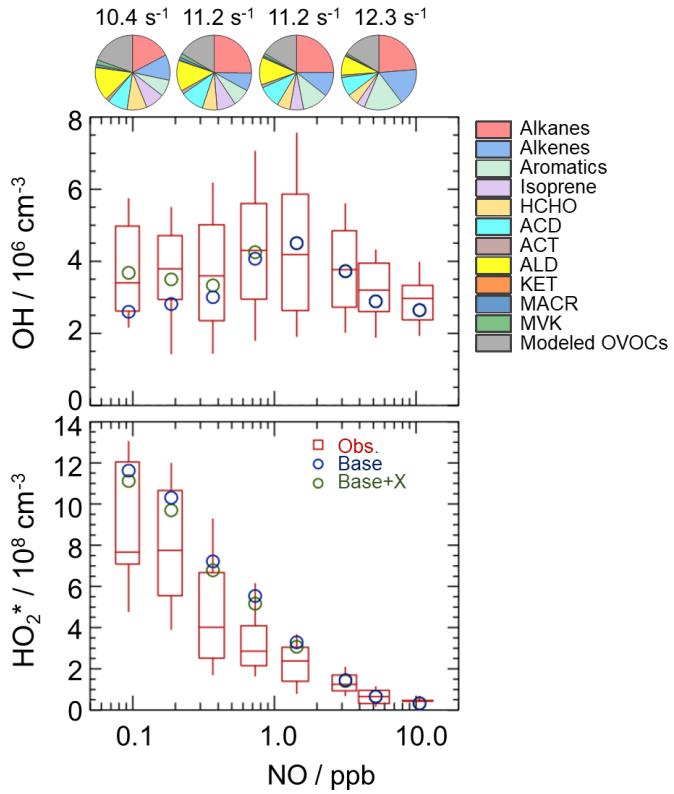

Figure 5: NO dependence of OH and HO_2^* radicals. The red box-whisker plots give the 10%, 25%, median, 75%, and 90% of the HOx observations. The blue circles show the median values of the HOx simulations by the base model, and the green circles show the HOx simulations by the model with X mechanism. Total VOCs reactivity and their organic speciation are presented by pie charts at the different NO intervals at the top. Only daytime values and NO concentration above the detection limit of the instrument were chosen. ACD and ACT denote acetaldehyde and acetone, respectively. ALD denotes the C3 and higher aldehydes. KET denotes ketones. MACR and MVK, which are both the isoprene oxidation products, denote methacrolein and methyl vinyl ketone, respectively.

5. The authors should clarify that the rate of ozone production shown in equation 2 (line 322) represents the gross instantaneous rate of ozone production rather than the net rate of ozone production, as it does not take into account any NO_2 formed that does not lead to O_3 production through the formation of HNO_3 from the OH + NO_2 reaction. In contrast Tan et al. (2017) appear to use the net rate of ozone production in their analysis of the chemistry at the Wangdu site. As a result, the comparison of the rate of ozone production between the sites shown in Figure 7c may not be an appropriate comparison. This should be clarified.

Reply

Thanks for your helpful suggestions. We calculated the net rate of ozone production and added the NO dependence of $P(O_3)$, AOC and the ratio of $P(O_3)$ to AOC in Fig. 7 (b-d).

Revision

(1) Section 4.4:

As the indictor for secondary pollution, net O_3 production rate, $P(O_3)$, can be calculated from

the O_3 formation rate ($F(O_3)$) and O_3 loss rate ($L(O_3)$), as shown in Eq. (3-5) (Tan et al., 2017). The diurnal profiles of the speciation $F(O_3)$ and $L(O_3)$ were shown in Fig. S5 in the Supplementary Information. The diurnal maxima of the modeled $F(O_3)$ and $L(O_3)$ were 18.9 ppb h^{-1} and 2.8 ppb h^{-1}, with the maximum $P(O_3)$ of 16.1 ppb h^{-1} at 11:00. The modeled $P(O_3)$ was comparable to that in Wangdu site in summer and much higher than that in Beijing in winter (Tan et al., 2018; Tan et al., 2017).

$$F(O_3) = k_{HO_2+NO}[HO_2][NO] + \sum_i k_{RO_2i+NO}[RO_2]_i[NO] \quad (3)$$

$$L(O_3) = \theta j(O^1D)[O_3] + k_{O_3+OH}[O_3][OH] + k_{O_3+HO_2}[O_3][HO_2] + (\sum(k^i_{alkenes+O_3}[alkenes^i]))[O_3] \quad (4)$$

$$P(O_3) = F(O_3) - L(O_3) \quad (5)$$

where θ is the fraction of O^1D from ozone photolysis that reacts with water vapor.

Herein, we presented the NO dependence of $P(O_3)$, AOC_{VOCs}, and ratio of $P(O_3)$ to AOC_{VOCs} in Fig. 7 (b-d), in which AOC_{VOCs} denotes the atmospheric oxidation capacity only from the VOCs oxidation. An upward trend $P(O_3)$ was presented with the increase of NO concentration when NO concentration was below 1 ppb, while a downward trend was shown with the increase of NO concentration when NO concentration was above 1 ppb. In terms of the NO dependence of AOC_{VOCs}, no significant variation was found, indicating VOCs oxidation was weakly impacted by NO concentrations in this campaign. Since AOC_{VOCs} can represent the VOCs oxidant rate, and thus the ratio of $P(O_3)$ to AOC_{VOCs} can reflect the yield of ozone production from VOCs oxidation. Similar to $P(O_3)$, the ratio increased with the increase of NO concentration when NO concentration was below 1 ppb. When NO concentration was above 1 ppb, the ratio decreased with the increase of NO concentration because NO_2 became the sink of OH radicals gradually. The maximum of the ratios existed when NO concentration was approximately 1 ppb, with a median of about 2, indicating the yield of ozone production from VOCs oxidation was about 2 in this study.

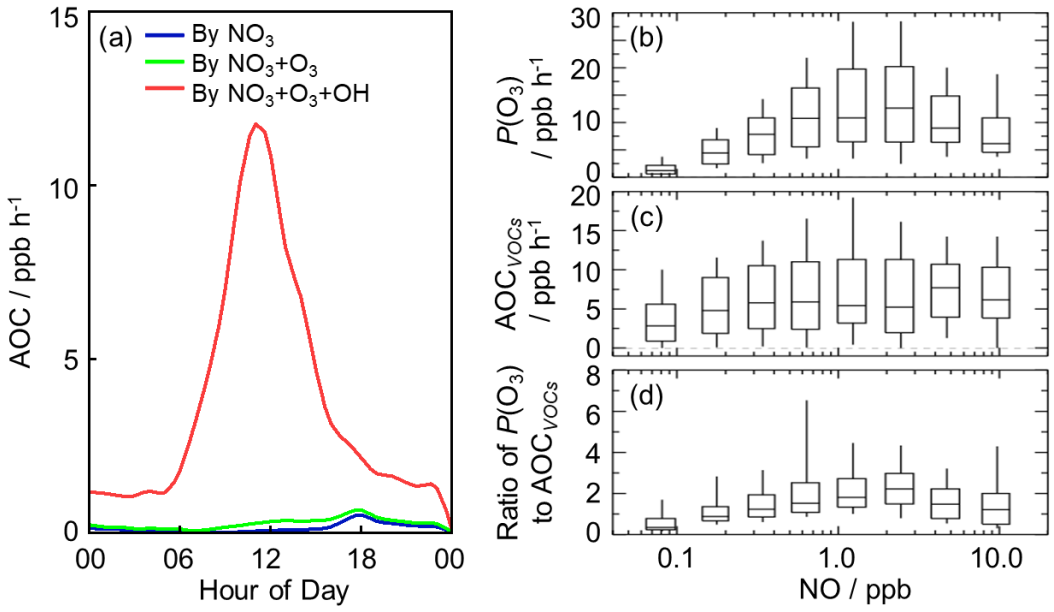

Figure 7: (a) The diurnal profiles of AOC in this campaign. (b) NO dependence of $P(O_3)$ during the daytime. (c) NO dependence of AOC_{VOCs} during the daytime, and AOC_{VOCs} denotes the atmospheric oxidation capacity only from the VOCs oxidation. (d) NO

dependence of the ratio of $P(O_3)$ to AOC_{VOCs} during the daytime. The box-whisker plots in (b-d) give the 10%, 25%, median, 75%, and 90% of $P(O_3)$, AOC and the ratio of $P(O_3)$ to AOC, respectively.

(2) The diurnal profiles of $P(O_3)$, $F(O_3)$, and $L(O_3)$ were added in Figure S5 in the Supplementary Information:

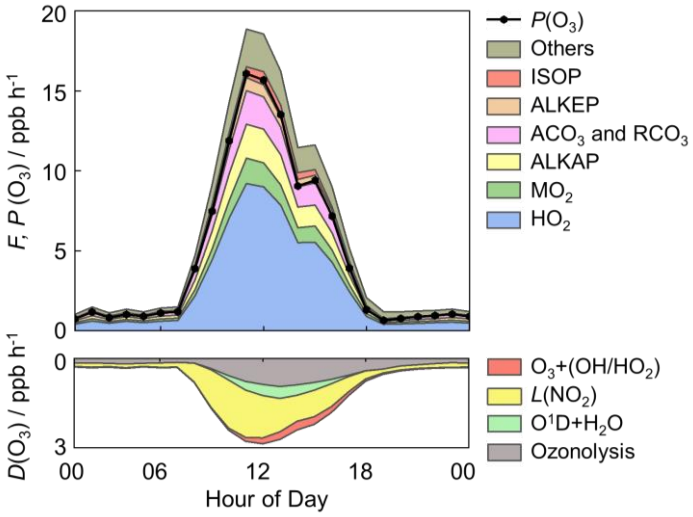

Figure S5: The diurnal profiles of $P(O_3)$, $F(O_3)$, and $L(O_3)$ in this campaign. The colored areas denote the speciation of $F(O_3)$ and $L(O_3)$ in the upper panel and lower panel, respectively. The black line denotes the $P(O_3)$, which is the discrepancy between $F(O_3)$ and $L(O_3)$. MO_2 denotes the methyl peroxy radicals. ALKAP, ALKEP and ISOP denote the RO_2 radicals derived from alkanes, alkenes and isoprene, respectively. ACO_3 denotes the acetyl peroxy radicals, and RCO_3 denotes the higher saturated acyl peroxy radicals.

References

Fuchs, H., Bohn, B., Hofzumahaus, A., Holland, F., Lu, K. D., Nehr, S., Rohrer, F., and Wahner, A.: Detection of HO2 by laser-induced fluorescence: calibration and interferences from RO2 radicals, Atmospheric Measurement Techniques, 4, 1209-1225, 10.5194/amt-4-1209-2011, 2011.

Fuchs, H., Tan, Z., Hofzumahaus, A., Broch, S., Dorn, H.-P., Holland, F., Kuenstler, C., Gomm, S., Rohrer, F., Schrade, S., Tillmann, R., and Wahner, A.: Investigation of potential interferences in the detection of atmospheric ROx radicals by laser-induced fluorescence under dark conditions, Atmospheric Measurement Techniques, 9, 1431-1447, 10.5194/amt-9-1431-2016, 2016.

Hofzumahaus, A., Rohrer, F., Lu, K., Bohn, B., Brauers, T., Chang, C.-C., Fuchs, H., Holland, F., Kita, K., Kondo, Y., Li, X., Lou, S., Shao, M., Zeng, L., Wahner, A., and Zhang, Y.: Amplified Trace Gas Removal in the Troposphere, Science, 324, 1702-1704, 10.1126/science.1164566, 2009.

Jones, C. E., Hopkins, J. R., and Lewis, A. C.: In situ measurements of isoprene and monoterpenes within a south-east Asian tropical rainforest, Atmospheric Chemistry and Physics, 11, 6971-6984, 10.5194/acp-11-6971-2011, 2011.

Lu, K. D., Hofzumahaus, A., Holland, F., Bohn, B., Brauers, T., Fuchs, H., Hu, M., Haeseler, R., Kita, K., Kondo, Y., Li, X., Lou, S. R., Oebel, A., Shao, M., Zeng, L. M., Wahner, A., Zhu, T., Zhang, Y. H., and Rohrer, F.: Missing OH source in a suburban environment near Beijing: observed and modelled OH and HO2 concentrations in summer 2006, Atmospheric Chemistry and Physics, 13, 1057-1080, 10.5194/acp-13-1057-2013, 2013.

Lu, K. D., Rohrer, F., Holland, F., Fuchs, H., Bohn, B., Brauers, T., Chang, C. C., Haeseler, R., Hu, M., Kita, K., Kondo, Y., Li, X., Lou, S. R., Nehr, S., Shao, M., Zeng, L. M., Wahner, A., Zhang, Y. H., and Hofzumahaus, A.: Observation and modelling of OH and HO2 concentrations in the Pearl River Delta 2006: a missing OH source in a VOC rich atmosphere, Atmospheric Chemistry and Physics, 12, 1541-1569, 10.5194/acp-12-1541-2012, 2012.

Mao, J., Ren, X., Zhang, L., Van Duin, D. M., Cohen, R. C., Park, J. H., Goldstein, A. H., Paulot, F., Beaver, M. R., Crounse, J. D., Wennberg, P. O., DiGangi, J. P., Henry, S. B., Keutsch, F. N., Park, C., Schade, G. W., Wolfe, G. M., Thornton, J. A., and Brune, W. H.: Insights into hydroxyl measurements and atmospheric oxidation in a California forest, Atmospheric Chemistry and Physics, 12, 8009-8020, 10.5194/acp-12-8009-2012, 2012.

Novelli, A., Hens, K., Ernest, C. T., Kubistin, D., Regelin, E., Elste, T., Plass-Duelmer, C., Martinez, M., Lelieveld, J., and Harder, H.: Characterisation of an inlet pre-injector laser-induced fluorescence instrument for the measurement of atmospheric hydroxyl radicals, Atmospheric Measurement Techniques, 7, 3413-3430, 10.5194/amt-7-3413-2014, 2014.

Stone, D., Evans, M. J., Walker, H., Ingham, T., Vaughan, S., Ouyang, B., Kennedy, O. J., McLeod, M. W., Jones, R. L., Hopkins, J., Punjabi, S., Lidster, R., Hamilton, J. F., Lee, J. D., Lewis, A. C., Carpenter, L. J., Forster, G., Oram, D. E., Reeves, C. E., Bauguitte, S., Morgan, W., Coe, H., Aruffo, E., Dari-Salisburgo, C., Giammaria, F., Di Carlo, P., and Heard, D. E.: Radical chemistry at night: comparisons between observed and modelled HOx, NO3 and N2O5 during the RONOCO project, Atmospheric Chemistry and Physics, 14, 1299-1321, 10.5194/acp-14-1299-2014, 2014.

Tan, Z., Lu, K., Hofzumahaus, A., Fuchs, H., Bohn, B., Holland, F., Liu, Y., Rohrer, F., Shao, M., Sun, K., Wu, Y., Zeng, L., Zhang, Y., Zou, Q., Kiendler-Scharr, A., Wahner, A., and Zhang, Y.: Experimental budgets of OH, HO2, and RO2 radicals and implications for ozone formation in the Pearl River Delta in China 2014, Atmospheric Chemistry and Physics, 19, 7129-7150, 10.5194/acp-19-7129-2019, 2019.

Tan, Z., Fuchs, H., Lu, K., Hofzumahaus, A., Bohn, B., Broch, S., Dong, H., Gomm, S., Haeseler, R., He, L., Holland, F., Li, X., Liu, Y., Lu, S., Rohrer, F., Shao, M., Wang, B., Wang, M., Wu, Y., Zeng, L., Zhang, Y., Wahner, A., and Zhang, Y.: Radical chemistry at a rural site (Wangdu) in the North China Plain: observation and model calculations of OH, HO2 and RO2 radicals, Atmospheric Chemistry and Physics, 17, 663-690, 10.5194/acp-17-663-2017, 2017.

Tan, Z., Rohrer, F., Lu, K., Ma, X., Bohn, B., Broch, S., Dong, H., Fuchs, H., Gkatzelis, G. I., Hofzumahaus, A., Holland, F., Li, X., Liu, Y., Liu, Y., Novelli, A., Shao, M., Wang, H., Wu, Y., Zeng, L., Hu, M., Kiendler-Scharr, A., Wahner, A., and Zhang, Y.: Wintertime photochemistry in Beijing: observations of ROx radical concentrations in the North China Plain during the BEST-ONE campaign, Atmospheric Chemistry and Physics, 18, 12391-12411, 10.5194/acp-18-12391-2018, 2018.

Yang, X., Lu, K., Ma, X., Liu, Y., Wang, H., Hu, R., Li, X., Lou, S., Chen, S., Dong, H., Wang, F., Wang, Y., Zhang, G., Li, S., Yang, S., Yang, Y., Kuang, C., Tan, Z., Chen, X., Qiu, P., Zeng, L., Xie, P., and Zhang, Y.: Observations and modeling of OH and HO2 radicals in Chengdu, China in summer 2019, The Science of the total environment, 772, 144829-144829, 10.1016/j.scitotenv.2020.144829, 2021.